Hindawi
Journal of Nanomaterials
Volume 2017, Article ID 4130569, 8 pages
https://doi.org/10.1155/2017/4130569

Research Article

Preparation of AuNPs/GQDs/SiO_2 Composite and Its Catalytic Performance in Oxidation of Veratryl Alcohol

Yaoyao Yang,[1,2] Jiali Zhang,[1] Fangwei Zhang,[1] and Shouwu Guo[1]

[1] *Department of Electronic Engineering, School of Electronic Information and Electrical Engineering, Shanghai Jiao Tong University, Shanghai 200240, China*
[2] *School of Materials Science and Engineering, University of Shanghai for Science and Technology, Shanghai 200093, China*

Correspondence should be addressed to Yaoyao Yang; yyyang@usst.edu.cn

Received 16 June 2017; Revised 12 September 2017; Accepted 18 October 2017; Published 9 November 2017

Academic Editor: Victor M. Castaño

Composites of gold nanoparticles and graphene quantum dots (AuNPs/GQDs) exhibit excellent dispersibility in aqueous solutions. Thus, it is difficult to separate them from wet reaction systems when they are used as catalysts. To resolve this issue, in this study, an AuNPs/GQDs composite was immobilized on silicon dioxide through the hydrothermal method, which involved the formation of an amide bond between the surface GQDs of the AuNPs/GQDs composite and the amino group of the silane. The as-synthesized AuNPs/GQDs/SiO_2 composite was found to be suitable for use as a heterogeneous catalyst for the oxidation of veratryl alcohol in water and exhibited catalytic activity comparable to that of bare AuNPs/GQDs as well as better recyclability.

1. Introduction

Graphene oxide (GO) and graphene quantum dots (GQDs) have attracted increasing attention in recent years, and early reports of gold nanoparticles (AuNPs)/GQDs composites appeared in 2013 and 2014. Generally, synthesis of these composites was carried out using several steps. In most cases, AuNPs and GQDs were modified separately before they were compounded [1–4]. However, other reports detailed the one-step generation of gold nanoparticles functionalized with graphene quantum dots (AuNPs/GQDs) [5, 6]. For example, GQDs with a two-dimensional lateral size of less than 100 nm, chloroauric acid ($HAuCl_4$), and sodium citrate were mixed, stirred, and heated to boiling in an aqueous solution to generate AuNPs/GQDs with uniform size [6]. Because the GQDs were obtained from the GO photo-Fenton reaction [7], they retained good chemical stability and the electron-conjugated state of GO. Further, they had more edge carboxyl groups, thus improving the stability and water dispersibility of AuNPs/GQDs. Studies of AuNPs/GQDs composites mainly focus on the field of gene detection [8, 9], biosensors [10, 11], and electrochemistry [12]. However, the very good water dispersibility of AuNPs/GQDs composites may result in great losses during circular catalytic reactions and this issue has not yet been addressed.

Silica (SiO_2) is used widely as the supporting matrix for catalysts owing to its unique physical/chemical properties, such as good thermal stability, large specific surface area, and good mechanical strength. Among the various types of silica available, mesoporous silica (such as MCM-41 and SBA-15), which has a high specific surface area and an ordered three-dimensional channel-like structure, has attracted even more attention in recent years [13–19]. For example, nanoparticles of certain noble metals can be supported on mesoporous silica by modifying the silanol bonds on their surfaces [20–22]. Accordingly, it can be assumed that AuNPs/GQDs [6] can be supported on silica and that doing so will improve their recyclability during the catalytic reaction. Thus, in this work, an AuNPs/GQDs/SiO_2 composite was designed, synthesized, and characterized for use as a catalyst for the oxidation of veratryl alcohol in aqueous solution.

2. Experiments

2.1. Materials. 3-Aminopropyltriethoxysilane (APTES, 99%, Aladdin), tetraethyl orthosilicate (TEOS, AR, Sinopharm

Chemical Reagent Co., Ltd.), Pluronic® F-127 polymer (Sigma Aldrich), ethanol (AR, Changshu Hongsheng Fine Chemical Co., Ltd.), hydrochloric acid (HCl, AR, Shanghai Ling Feng Chemical Reagent Co., Ltd.), chloroauric acid ($HAuCl_4$, 48–50% Au basis, Aladdin), sodium citrate (dihydrate, Shanghai Shisihewei Chemical Co., Ltd.), and hydrogen peroxide (H_2O_2, 30%, Shanghai Ling Feng Chemical Reagent Co., Ltd.) were used directly after purchase. The graphene oxide (GO) and GQDs samples used were prepared as per previously reported procedures [7, 23].

2.2. Preparation of AuNPs/GQDs Aqueous Suspension. First, the AuNPs/GQDs composite was prepared according to the method reported in our previous study [6]. In brief, 10 mg of the GQDs (10 mg/mL GQD solution, 1 mL), 20 mg $HAuCl_4$ (2% w/w aqueous solution of chloroauric acid, 1 g), and 5 mL of deionized water were added to a 50 mL flask, which was placed in a 100°C oil bath, and stirred. Then, 10 mL of a sodium citrate solution (58.8 mg of sodium citrate and 10 mL of deionized water) was added to the flask immediately. The flask was kept at 100°C to prepare the GQDs-functionalized gold nanoparticles (i.e., AuNPs/GQDs composite). The flask was removed from the oil bath after 30 min, and the solution in the flask was transferred to a 25 mL volumetric flask. The volume was adjusted to 25 mL by adding deionized water. The thus-obtained dispersion of the AuNPs/GQDs was then left to rest.

2.3. Synthesis of AuNPs/GQDs/SiO_2. First, 1.26 g of TEOS, 8.4 g of APTES, and 20 mL of ethanol were stirred at 40°C for 1 h. Next, a Pluronic F-127 solution (0.38 g of F127, 2 mL of HCl, and 20 mL of ethanol) and 24 mL of the AuNPs/GQDs dispersion were added to this mixture. The reaction was allowed to occur for 1 h at 80°C. Then, the temperature was increased to 100°C, and the mixture was refluxed for 24 h. Finally, the hydrothermal treatment was performed on the mixture at 150°C for 24 h. This yielded a black solid product (AuNPs/GQDs/SiO_2), which was washed thrice with deionized water and dried in a vacuum drier at 60°C for 12 h.

2.4. Characterization of Synthesized Composite. Atomic force microscopy (AFM, Multimode Nanoscope V, Veeco Instrumental Co. Ltd., USA), transmission electron microscopy (TEM, JEOL JEM-2100, Japan), field-emission scanning electron microscopy (FE-SEM, ZEISS ULTRA 55, Germany), Fourier transform infrared spectroscopy (FT-IR, Bruker EQUINOX 55, Germany), surface area and porosity measurements (Micromeritics Instrument Corp., ASAP 2460, USA), X-ray photoelectron spectroscopy (XPS, Kratos Analytical axis Untra DLD, UK), and X-ray diffraction (XRD, Bruker D8 Advance, Germany) measurements were performed to characterize the morphology of the synthesized composite. In addition, high-performance liquid chromatography (HPLC, Agilent Technologies 1220 infinity LC, Germany) and ultraviolet-visible (UV-vis) spectroscopy (Shimadzu UV-2550, Japan) were performed to calculate the oxidation yield after the catalytic reaction.

2.5. Oxidation of Veratryl Alcohol in Aqueous Solution. The catalytic performance of the obtained composite was evaluated based on the oxidation of veratryl alcohol in an aqueous solution. The standard reaction conditions were as follows: 2 μmol of veratryl alcohol, 20 μmol of hydrogen peroxide, 1 mL of deionized water, and 2 mg of the synthesized composite were added to a 5 mL centrifuge tube. The centrifuge tube was then shaken at a temperature of 50°C for different amounts of time. After the reaction, 2 mL deionized water was added to stop the reaction and then the composite catalyst was removed by centrifugation at 10,000 rpm for 15 min. The solutions were diluted to 10 mL for UV-vis measurement. The conversion ratio of the reaction was calculated from the UV-vis test and averaged over three independent experiments.

3. Result and Discussion

3.1. Morphology of AuNPs/GQDs/SiO_2 Composite. First, the particle size and morphology of the AuNPs/GQDs composite were determined using AFM imaging (Figure 1(a)). The size of the composite particles as estimated from the AFM images was mainly in 5–10 nm; this was confirmed by TEM imaging as well (Figures 1(b) and 1(d)). HRTEM image (Figure 1(c)) showed the lattice parameters of 0.124 nm and 0.243 nm which were corresponding to Au (311) lattice plane [24] and GQDs (111) lattice plane [25], respectively. These TEM images revealed the structure of AuNPs/GQDs in detail; the GQDs are attached on the surfaces of the AuNPs same as our previous study [6], though the sickness of GQDs layer (the edge of particles in Figure 1(b)) is much thinner due to the lower feed ratio than before; it is likely that the attached GQDs prevented AuNPs from further aggregation. The as-prepared AuNPs/GQDs composite was used as the raw material to synthesize the AuNPs/GQDs/SiO_2 composite. In principle, the GQDs used in this study, which were synthesized by the photo-Fenton reaction, would have contained unbound carboxylic groups, which can be activated by the hydrochloric acid in the reaction solution. Therefore, the activated GQDs on the surfaces of the AuNPs/GQDs particles could react with the amino groups of APTES during the reflux and hydrothermal processes. This was probably the main step in the bonding of the AuNPs/GQDs particles on the SiO_2 support.

To confirm whether this was indeed the case, FT-IR and XPS measurements were performed, in order to further analyze the AuNPs/GQDs/SiO_2 composite. As shown in Figure 2(a), peaks related to the stretching vibrations of the N–H bond (amino, 3400 cm^{-1} and 3500 cm^{-1}), C–N bond (1420 to 1400 cm^{-1}), and Si-O bond (798 cm^{-1}) can be observed clearly in the FT-IR spectrum of APTES. Further, peaks ascribable to the stretching vibrations of the N–H bond (amido, 3350 cm^{-1} and 3180 cm^{-1}) and C=O bond (1630 cm^{-1}) can be seen in the spectrum of the AuNPs/GQDs/SiO_2 composite (Figure 2(b)), confirming the formation of the amide bond. In addition, the fact that the intensity of the peak related to the Si–O bond (798 cm^{-1}) decreased and the peak related to the Si–O–Si bond (1083 cm^{-1}) remained unchanged confirmed the formation of the SiO_2 support.

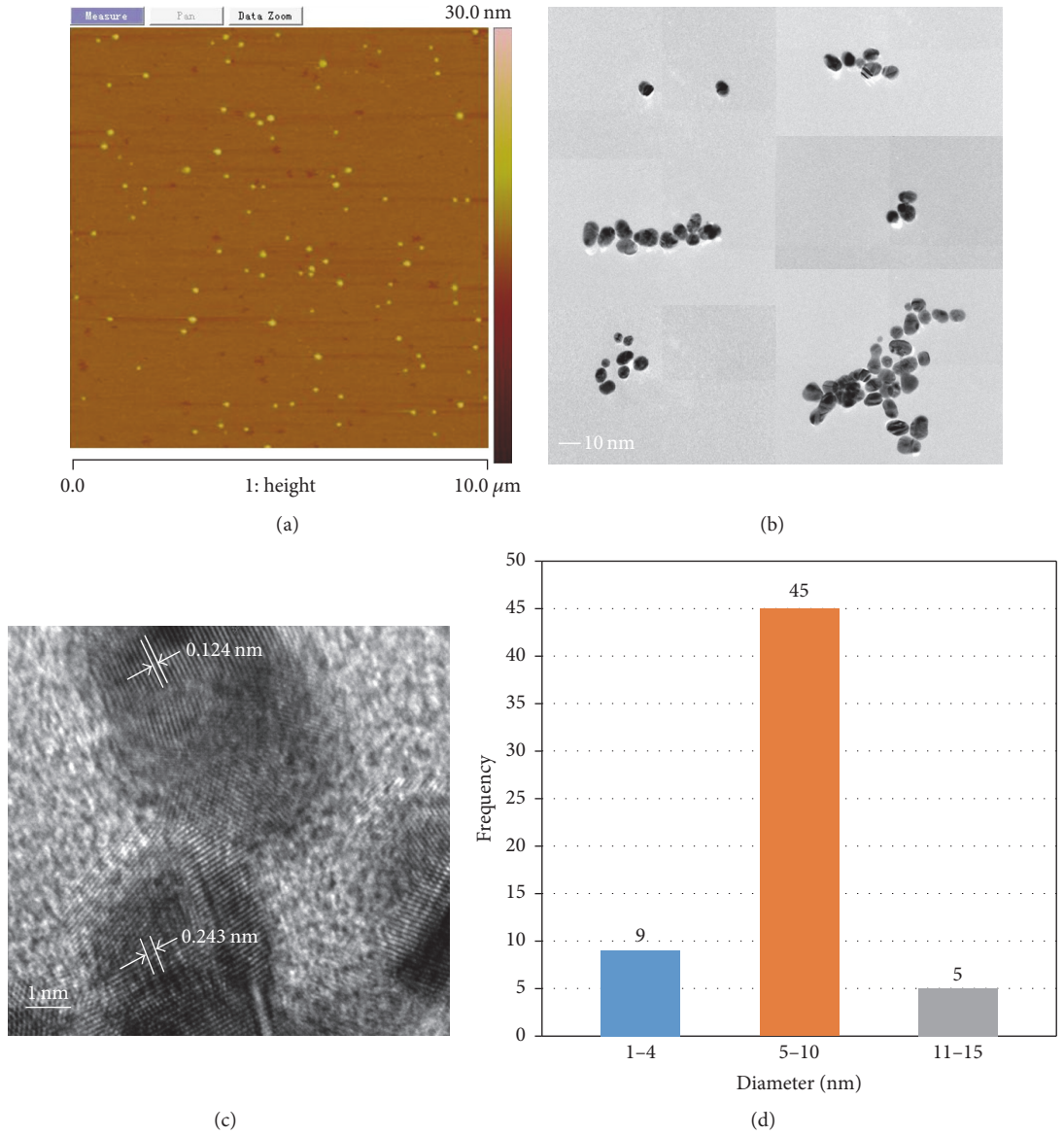

Figure 1: AFM, TEM, HRTEM images, and particle size distribution of AuNPs/GQDs.

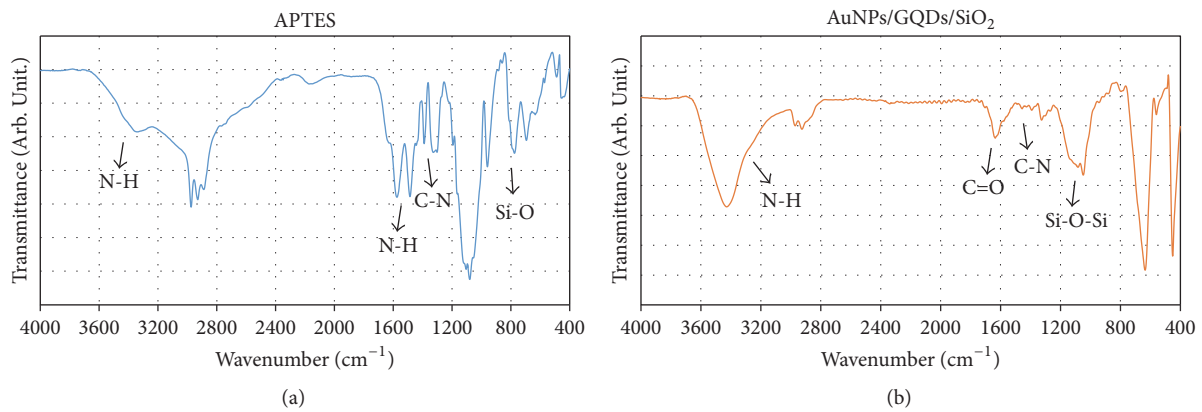

Figure 2: FT-IR spectra of APTES and AuNPs/GQDs/SiO_2, determined using KBr tablets.

Table 1: Concentrations of constituent elements of AuNPs/GQDs/SiO_2, as determined by XPS measurements.

Element	C 1s	N 1s	O 1s	Si 2p	Au 4f
Atomic Conc. (%)	59.2	6.22	24.3	9.35	0.92
Mass Conc. (%)	43.6	5.34	23.9	16.1	11.1

Table 2: Catalytic ability of AuNPs/GQDs/SiO_2 with respect to oxidation of veratryl alcohol.

Yield of veratraldehyde (%)[a]	1st run	2nd run	3rd run	4th run	5th run
UV-vis[b]	45.4 (±10.1)	84.0 (±7.14)	85.1 (±5.44)	83.3 (±7.39)	77.7 (±5.95)
HPLC[c]	35.4	62.7	70.0	65.8	75.3

[a]Reaction conditions: 2 μmol of veratryl alcohol, 20 μmol of hydrogen peroxide, 1 mL of deionized water, 2 mg of composite, and temperature of 50°C. The standard curve whose x-coordinate is the conversion ratio and y-coordinate is the UV absorbance is shown in Fig. S2b. [b]Conversion ratios are the average values for three reaction runs. [c]The peak area of the HPLC curve for a 2 mmol/L veratraldehyde solution (corresponding to 100% conversion) is 8584 mAU × S.

The concentrations of the constituent elements of the AuNPs/GQDs/SiO_2 composite, determined from the XPS measurements, are shown in Table 1. Further, the C 1s, N 1s, O 1s, Si 2p, and Au 4f spectra are shown in Figure 3. The C 1s spectra indicated that the binding energy for the C–C and C=C bonds was 284.7 eV, while those for the C–N, C–Si, C=O, and C–O bonds were 285.9 eV, 284.0 eV, 288.3 eV, and 287.6 eV, respectively. These results further confirmed the formation of an amide bond between the GQDs and SiO_2.

Next, the morphology and size of the AuNPs/GQDs/SiO_2 composite were analyzed through FE-SEM, TEM, and XRD measurements. The FE-SEM image in Figure 4(a) shows clearly that the AuNPs/GQDs/SiO_2 composite has a three-dimensional continuous structure. By measuring the surface area and porosity of the AuNPs/GQDs/SiO_2 composite, its BET surface was determined and found to be approximately 64.7 $m^2\ g^{-1}$. Further, the pores of the composite were 5–50 nm in size (as shown in Fig. S1b in Supplementary Material available online at https://doi.org/10.1155/2017/4130569). Figures 4(b) and 4(c) are TEM and HRTEM images of the AuNPs/GQDs/SiO_2 composite, respectively, and further confirm that the AuNPs/GQDs particles are embedded in the SiO_2 support. Finally, the XRD pattern of the AuNPs/GQDs/SiO_2 composite exhibits peaks of 2θ at 38.1°, 44.4°, 64.6°, and 77.6°; these correspond to the (111), (200), (220), and (311) planes, respectively, of gold crystallites and confirm the existence of AuNPs [26].

3.2. Catalytic Performance of As-Prepared AuNPs/GQDs/SiO_2 Composite. It is well known that Au nanoparticles supported on various matrices can be employed to catalyze alcohol oxidation [27]. In this work, oxidation of veratryl alcohol in an aqueous solution using H_2O_2 as an oxidizing agent was employed as a model system. The catalytic performance of the synthesized AuNPs/GQDs/SiO_2 composite with respect to the oxidation of veratryl alcohol was evaluated through UV-vis spectroscopy and HPLC measurements. The characteristic UV-vis absorption peaks of veratryl alcohol, veratraldehyde, and veratric acid appear at 277 nm, 308 nm, and 252 nm, respectively (Fig. S2a). As shown in Figure 5(a), with an increase in the reaction time, the veratraldehyde yield increased gradually. The spectra acquired after reaction times of 6 h, 9 h, and 12 h indicated that the conversion of the alcohol to the aldehyde was almost complete within 9 h and that the conversion of the aldehyde to the acid started subsequently. For durations of 27 h and 42 h, the generated veratraldehyde of oxidation reaction catalyzed by AuNPs/GQDs/SiO_2 composite was then partly converted into veratric acid; this trend is well consistent with our previous work [6]. It was generally accepted that the residual oxygen-containing functional groups on the surface of supported Au catalysts play a key role in their catalytic performances, especially for the oxidization reactions [28]. Besides, it was also reported that the GQDs with plenty of the periphery carboxylic groups show high peroxidase-like activity under acidic environment [29]. Thus, the mechanism of the oxidation reaction catalyzed by AuNPs/GQDs/SiO_2 composite is summarized as follows. During the reaction, veratryl alcohol was absorbed onto the AuNPs/GQDs through p–p stacking firstly; then, the superoxide anion $O_2^{-\bullet}$ and singlet oxygen $^1O_2$ generated by both AuNPs and GQDs with H_2O_2 oxidize the reactant to veratraldehyde and veratric acid. The selectivity and conversion efficiency of AuNPs/GQDs/SiO_2 composite are mainly contributed by AuNPs, GQDs and their interaction.

To evaluate the recyclability of the AuNPs/GQDs/SiO_2 composite catalyst, after the 2 h reaction, the composite was separated from the reaction system by centrifugation at 10,000 rpm for 15 min, and the reaction products were analyzed. This process was repeated four times. As shown in Figure 5(b), the yield of veratraldehyde remained constant (over 80%) from the second cycle onwards; these results are listed in Table 2. Thus, it was confirmed that, when used as a catalyst, the as-prepared AuNPs/GQDs/SiO_2 composite exhibited greater reusability as compared to the AuNPs/GQDs composite, which cannot be separated from the reaction system by centrifugation. Besides, TEM images suggest that the morphology of the AuNPs/GQDs/SiO_2 composite underwent almost no change, as shown in Figure 6.

4. Conclusion

AuNPs/GQDs were immobilized on silicon dioxide through the hydrothermal method, which involved the formation of

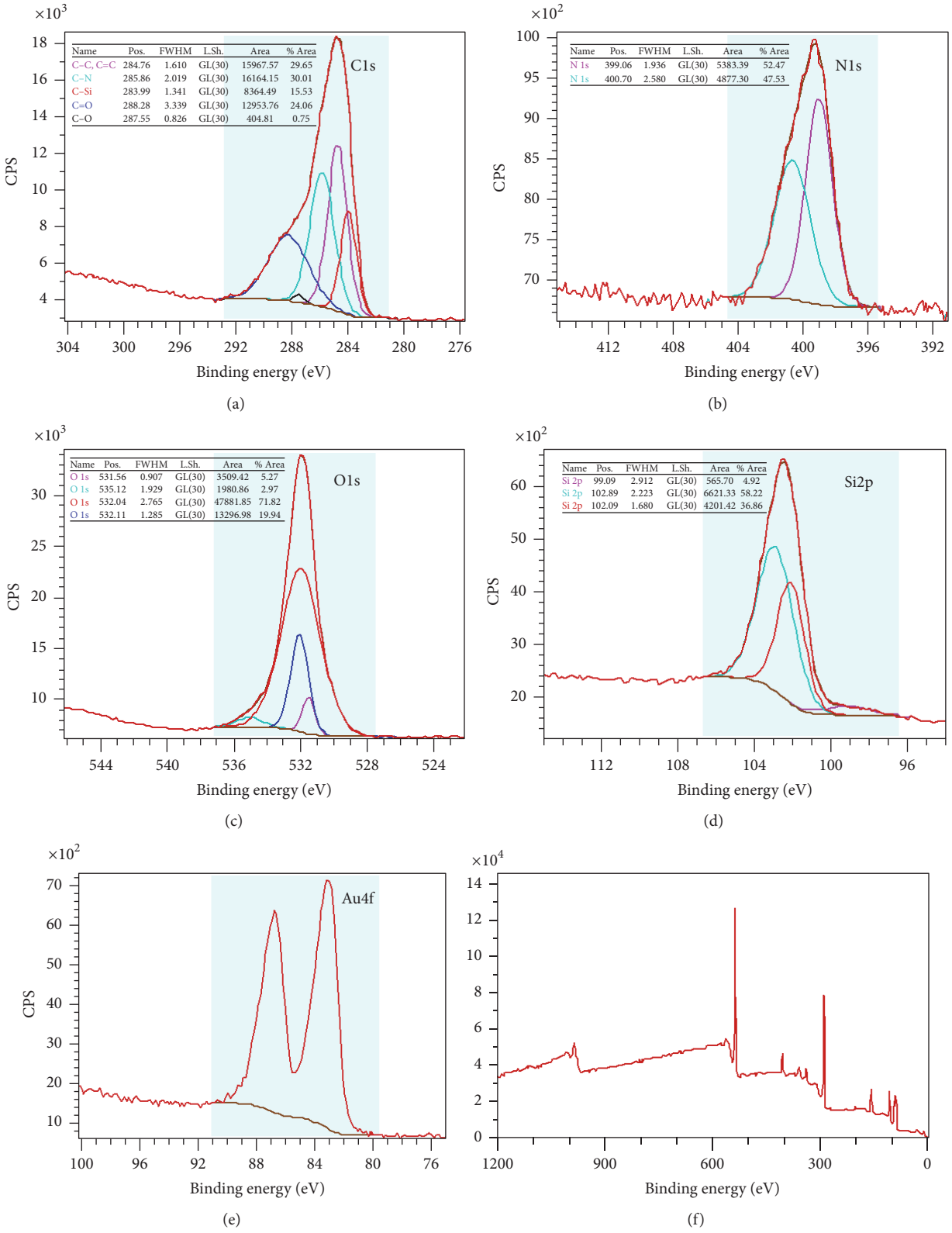

Figure 3: XPS spectra of AuNPs/GQDs/SiO_2.

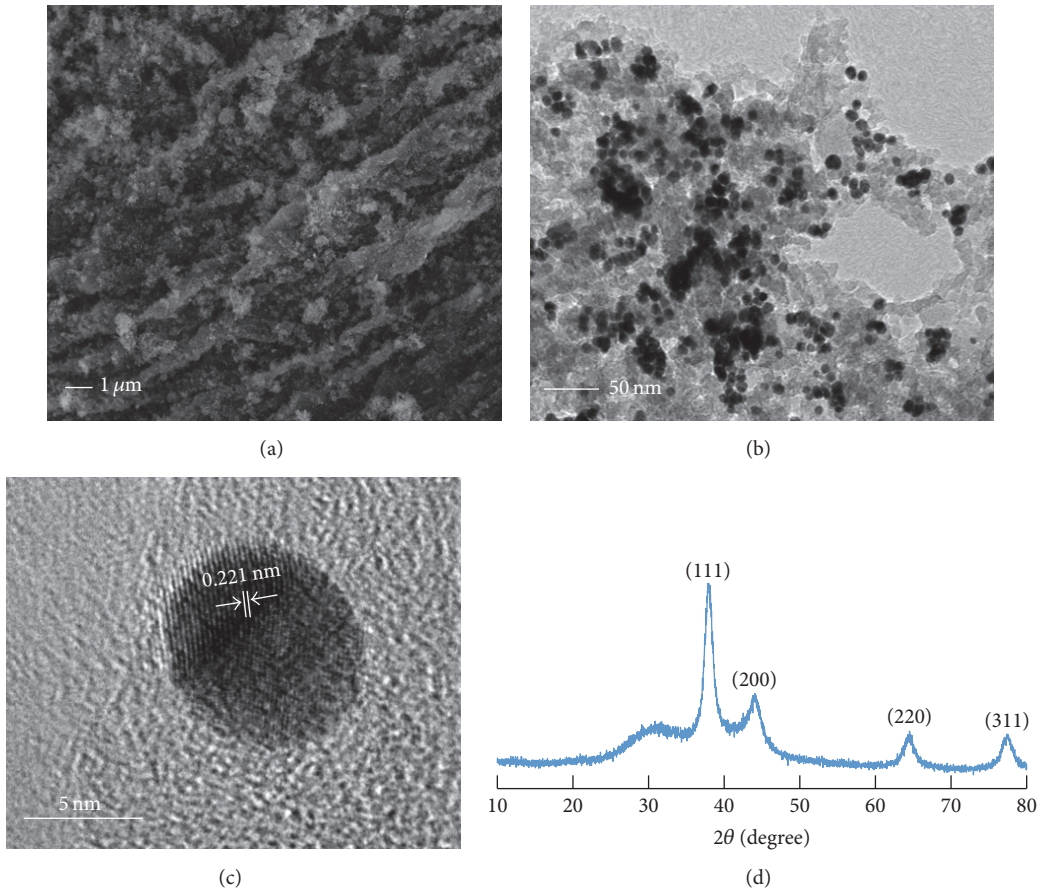

Figure 4: FE-SEM image, TEM image, and XRD spectrum of AuNPs/GQDs/SiO_2 composite.

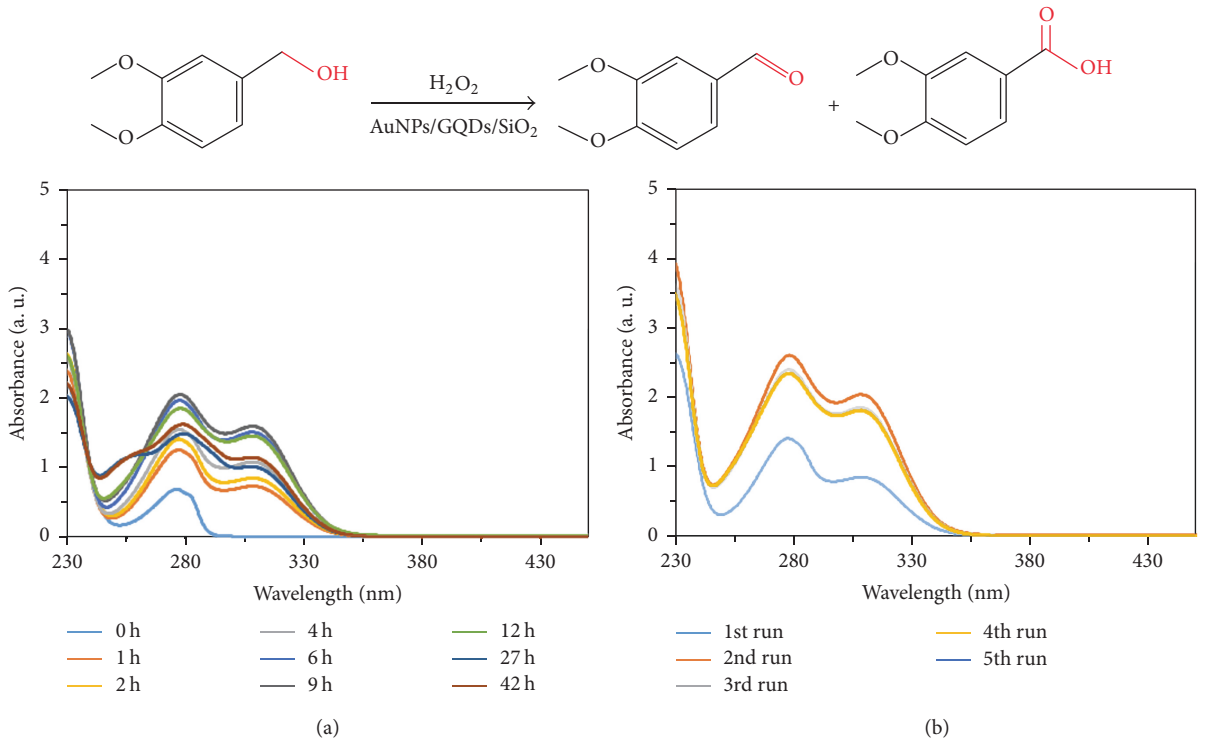

Figure 5: UV-vis spectra of aqueous solutions containing veratryl alcohol after being subjected to the catalytic oxidation reaction for various durations. Reaction conditions: 2 μmol of veratryl alcohol, 20 μmol of hydrogen peroxide, 1 mL of deionized water, 2 mg of composite, and temperature of 50°C.

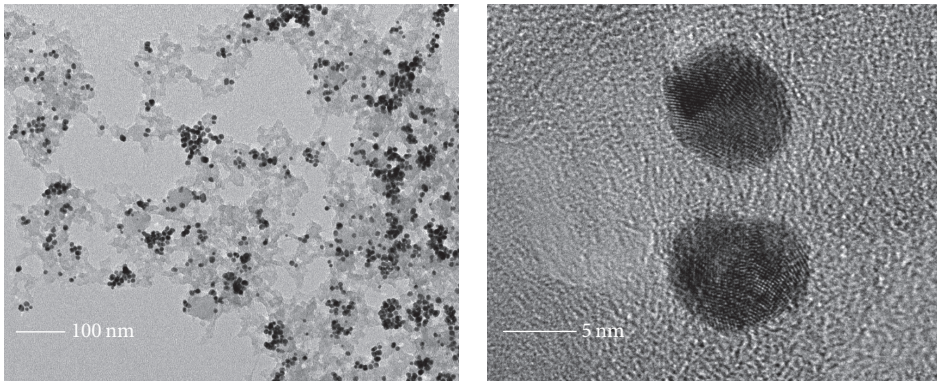

(a) (b)

Figure 6: TEM image and HTEM image of AuNPs/GQDs/SiO_2 composite after five circular catalytic reactions.

an amide bond between the surface GQDs and the silane. The as-obtained AuNPs/GQDs/SiO_2 composite exhibited a surface area of 64.7 $m^2 g^{-1}$ and had a good dispersion of AuNPs/GQDs. Using the AuNPs/GQDs/SiO_2 composite as a heterogeneous catalyst and hydrogen peroxide as the oxidant, veratryl alcohol could be oxidized to veratraldehyde and veratric acid in a step-wise manner. It was also confirmed that the recyclability of the AuNPs/GQDs composite improved after immobilization on SiO_2. Work is in progress to obtain insight into the details regarding the morphology and catalytic performance of AuNPs/GQDs/SiO_2 composites fabricated under a wider range of conditions.

Conflicts of Interest

The authors declare that they have no conflicts of interest.

Acknowledgments

This work was financially supported by the National "973 Program" of China (nos. 2014CB260411 and 2015CB931801) and the National Science Foundation of China (no. 11374205).

References

[1] L. Wang, J. Zheng, S. Yang et al., "Two-Photon Sensing and Imaging of Endogenous Biological Cyanide in Plant Tissues Using Graphene Quantum Dot/Gold Nanoparticle Conjugate," *ACS Applied Materials & Interfaces*, vol. 7, no. 34, pp. 19509–19515, 2015.

[2] J. Shi, C. Chan, Y. Pang et al., "A fluorescence resonance energy transfer (FRET) biosensor based on graphene quantum dots (GQDs) and gold nanoparticles (AuNPs) for the detection of mecA gene sequence of Staphylococcus aureus," *Biosensors and Bioelectronics*, vol. 67, pp. 595–600, 2015.

[3] J. Liu, X. He, K. Wang et al., "A highly sensitive electrochemiluminescence assay for protein kinase based on double-quenching of graphene quantum dots by G-quadruplex-hemin and gold nanoparticles," *Biosensors and Bioelectronics*, vol. 70, pp. 54–60, 2015.

[4] S. L. Ting, S. J. Ee, A. Ananthanarayanan, K. C. Leong, and P. Chen, "Graphene quantum dots functionalized gold nanoparticles for sensitive electrochemical detection of heavy metal ions," *Electrochimica Acta*, vol. 172, pp. 7–11, 2015.

[5] Y. Guo, W. Li, M. Zheng, and Y. Huang, "Facile preparation of graphene dots functionalized au nanoparticles and their application as peroxidase mimetics in glucose detection," *Acta Chimica Sinica*, no. 6, pp. 713–719, 2014.

[6] X. Wu, S. Guo, and J. Zhang, "Selective Oxidation of Veratryl Alcohol with Composites of Au Nanoparticles and Graphene Quantum Dots as Catalysts," *Chemical Communications*, vol. 51, pp. 6318–6321, 2015.

[7] X. Zhou, Y. Zhang, C. Wang et al., "Photo-Fenton reaction of graphene oxide: A new strategy to prepare graphene quantum dots for DNA cleavage," *ACS Nano*, vol. 6, no. 8, pp. 6592–6599, 2012.

[8] Q. Lu, W. Wei, Z. Zhou, Y. Zhang, and S. Liu, "Electrochemiluminescence resonance energy transfer between graphene quantum dots and gold nanoparticles for DNA damage detection," *Analyst*, vol. 139, pp. 2404–2410, 2014.

[9] J. Qian, K. Wang, C. Wang et al., "A FRET-based ratiometric fluorescent aptasensor for rapid and onsite visual detection of ochratoxin A," *Analyst*, vol. 140, pp. 7434–7442, 2015.

[10] J. Shi, F. Tian, J. Lyu, and M. Yang, "Nanoparticle based fluorescence resonance energy transfer (FRET) for biosensing applications," *Journal of Materials Chemistry B*, vol. 3, pp. 6989–7005, 2015.

[11] Y. Dong, H. Wu, P. Shang, X. Zeng, and Y. Chi, "Immobilizing water-soluble graphene quantum dots with gold nanoparticles for a low potential electrochemiluminescence immunosensor," *Nanoscale*, vol. 7, no. 39, pp. 16366–16371, 2015.

[12] M. Mazloum-Ardakani, R. Aghaei, M. Abdollahi-Alibeik, and A. Moaddeli, "Fabrication of modified glassy carbon electrode using graphene quantum dot, gold nanoparticles and 4-(((4-mercaptophenyl)imino)methyl) benzene-1,2-diol by self-assembly method and investigation of their electrocatalytic activities," *Journal of Electroanalytical Chemistry*, vol. 738, pp. 113–122, 2015.

[13] M. A. Sibeko, M. L. Saladino, A. S. Luyt, and E. Caponetti, "Morphology and properties of poly(methyl methacrylate) (PMMA) filled with mesoporous silica (MCM-41) prepared by melt compounding," *Journal of Materials Science*, vol. 51, no. 8, pp. 3957–3970, 2016.

[14] W. Chen, X. Li, Z. Pan, S. Ma, and L. Li, "Effective mineralization of Diclofenac by catalytic ozonation using Fe-MCM-41 catalyst," *Chemical Engineering Journal*, vol. 304, pp. 594–601, 2016.

[15] W. A. Talavera-Pech, A. Esparza-Ruiz, P. Quintana-Owen, A. R. Vilchis-Nestor, C. Carrera-Figueiras, and A. Ávila-Ortega, "Effects of different amounts of APTES on physicochemical and structural properties of amino-functionalized MCM-41-MSNs," *Journal of Sol-Gel Science and Technology*, vol. 80, no. 3, pp. 697–708, 2016.

[16] A. Kumar, V. P. Kumar, V. Vishwanathan, and K. V. R. Chary, "Synthesis, characterization, and reactivity of Au/MCM-41 catalysts prepared by homogeneous deposition-precipitation (HDP) method for vapor phase oxidation of benzyl alcohol," *Materials Research Bulletin*, vol. 61, pp. 105–112, 2014.

[17] Y. Chen, J. Wang, W. Li, and M. Ju, "Microwave-assisted hydrothermal synthesis of Au/TiO_2/SBA-15 for enhanced visible-light photoactivity," *Materials Letters*, vol. 159, pp. 131–134, 2015.

[18] T. Wang, X. Yuan, S. Li, L. Zeng, and J. Gong, "CeO_2-modified Au@ SBA-15 nanocatalysts for liquid-phase selective oxidation of benzyl alcohol," *Nanoscale*, vol. 7, no. 17, pp. 7593–7602, 2015.

[19] H.-C. Wu, T.-C. Chen, N.-C. Lai et al., "Synthesis of sub-nano-sized Pt particles on mesoporous SBA-15 material and its application to the CO oxidation reaction," *Nanoscale*, vol. 7, no. 40, pp. 16848–16859, 2015.

[20] J. N. Kuhn, W. Huang, C.-K. Tsung, Y. Zhang, and G. A. Somorjai, "Structure sensitivity of carbon-nitrogen ring opening: Impact of platinum particle size from below 1 to 5 nm upon pyrrole hydrogenation product selectivity over monodisperse platinum nanoparticles loaded onto mesoporous silica," *Journal of the American Chemical Society*, vol. 130, no. 43, pp. 14026-14027, 2008.

[21] C. A. Witham, W. Huang, C.-K. Tsung, J. N. Kuhn, G. A. Somorjai, and F. D. Toste, "Converting homogeneous to heterogeneous in electrophilic catalysis using monodisperse metal nanoparticles," *Nature Chemistry*, vol. 2, no. 1, pp. 36–41, 2010.

[22] E. Gross, J. H. Liu, S. Alayoglu et al., "Asymmetric catalysis at the mesoscale: Gold nanoclusters embedded in chiral self-assembled monolayer as heterogeneous catalyst for asymmetric reactions," *Journal of the American Chemical Society*, vol. 135, no. 10, pp. 3881–3886, 2013.

[23] J. Zhang, H. Yang, G. Shen, P. Cheng, and S. Guo, "Reduction of graphene oxide via L-ascorbic acid," *Chemical Communications*, vol. 46, pp. 1112–1114, 2010.

[24] J. D. Hayawalt, H. W. Rinn, and L. K. Frevel, "Chemical Analysis by X-Ray Diffraction Classification and Use of X-Ray Diffraction Patterns," *Industrial and Engineering Chemistry, Analytical Edition*, vol. 10, no. 9, pp. 457–512, 1938.

[25] C. Cheng, M. Li, and Q. Wu, "Development in, characterization of graphene quantum dots," *Journal of Functional Materials*, vol. 4, no. 48, pp. 4033–4040, 2017.

[26] V. M. Kariuki, I. Yazgan, A. Akgul, A. Kowal, M. Parlinskad, and O. A. Sadik, "Synthesis and catalytic, antimicrobial and cytotoxicity evaluation of gold and silver nanoparticles using biodegradable, Π-conjugated polyamic acid," *Environmental Science: Nano*, vol. 2, pp. 518–527, 2015.

[27] C. D. Pina, E. Falletta, and M. Rossi, "Update on selective oxidation using gold," *Chemical Society Reviews*, vol. 41, pp. 350–369, 2012.

[28] J. Zhu, S. A. C. Carabineiro, D. Shan, J. L. Faria, Y. Zhu, and J. L. Figueiredo, "Oxygen activation sites in gold and iron catalysts supported on carbon nitride and activated carbon," *Journal of Catalysis*, vol. 274, no. 2, pp. 207–214, 2010.

[29] Y. Zhang, C. Wu, X. Zhou et al., "Graphene quantum dots/gold electrode and its application in living cell H_2O_2 detection," *Nanoscale*, vol. 5, no. 5, pp. 1816–1819, 2013.